# An energy theory of glaucoma

Ying Li[a], Daqing Li[a], Xi Ying[b], Peng T Khaw[c] and Geoffrey Raisman[a]

a Spinal Research Unit, Department of Brain Repair and Rehabilitation, UCL Institute of Neurology, WC1N 3BG, London, UK

b Southwest Hospital/Southwest Eye Hospital, Third Military Medical University, Chongqing 400038, China.

c NIHR Biomedical Research Centre Moorfields Eye Hospital and UCL Institute of Ophthalmology

For correspondence Mailing address:
Dr Geoffrey Raisman
Spinal Research Unit
Department of Brain Repair and Rehabilitation
UCL Institute of Neurology
Queen Square
London WC1N 3BG
UK
G.Raisman@ucl.ac.uk

RUNNING TITLE: An Energy Theory of Glaucoma

Number of words:

| | |
|---|---|
| Abstract: | 203 |
| Introduction: | 294 |
| Methods: | 452 |
| Results: | 2623 |
| Discussion: | 3147 |
| Bibliography: | 1743 |
| Legends: | 2031 |

Correspondence to:
G. Raisman@ucl.ac.uk
+44 207 676 2172

Main Points

A fluid filled space around the rim of the ONH buffers intraocular pressure.

Glaucoma overwhelms the energy capacity of the buffer.

Uncontrolled backward stretching of the blood vessels results in ischaemic death of the glial cells leading to axotomy.

Graphical Abstract:

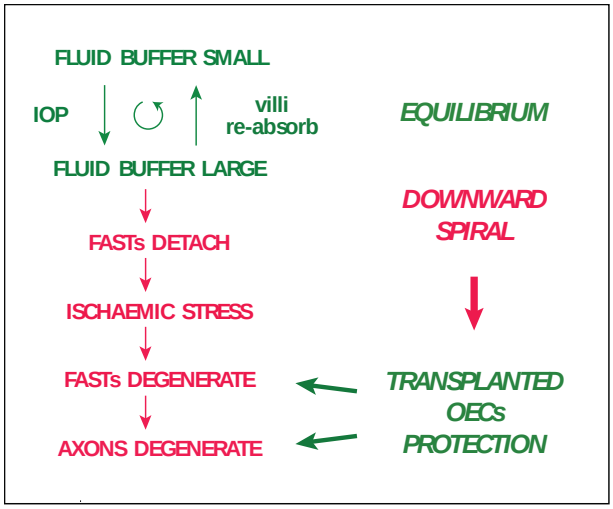
FLUID BUFFER SMALL
IOP
villi
re-absorb
EQUILIBRIUM
FLUID BUFFER LARGE
DOWNWARD
SPIRAL
FASTs DETACH
ISCHAEMIC STRESS
FASTs DEGENERATE
TRANSPLANTED
OECs
PROTECTION
AXONS DEGENERATE

KEY WORDS

OPTIC NERVE HEAD
INTRAOCULAR PRESSURE
GLIA
OLFACTORY ENSHEATHING CELLS
POSTERIOR CILIARY ARTERY

ABSTRACT

A radial array of fortified astrocytes (FASTs) is the load bearing structure of the rat optic nerve head (ONH). At the retinal end the ONH is suspended on a fluid filled extracellular space occupied by modified pigment cells which generate a glomerular-like formation of villi. We propose that regulation of fluid in and out of this space may contribute to buffering the normal fluctuations of intraocular pressure. The energy requirement for the fluid transfer process is provided by the dense vascularity of the ONH and is reflected in the giant mitochondria of the FASTs. We propose that glaucoma occurs when a maintained rise in pressure overwhelms the capacity of this regulatory system. Under these circumstances the FAST array becomes detached from its anchorage in the surrounding ONH sheath. Progressively driven backwards by the pressure, the FASTs degenerate. We propose that the degeneration of the FASTs is associated with ischaemic damage caused by the backward stretching of their blood supply. Retraction of the FAST processes deprives the retinal ganglion cell axons of their energy support, resulting in axotomy. We consider that our previously observed rescue of axons and FASTs by transplantation of olfactory ensheathing cells is due to replacement of this lost energy source.

## INTRODUCTION

Glaucoma damages the axons of the retinal ganglion cells (RGCs) where they exit the eyeball by passing through the scleral deficit at the optic disc (Morrison, Johnson, and Cepurna, 2008;Quigley, 2011;Howell, Libby, Jakobs, Smith, Phalan, Barter, Barbay, Marchant, Mahesh, Porciatti, Whitmore, Masland, and John, 2007). This specialised region is known as the optic nerve head (ONH).

In primates, including man, the tissue of the ONH consists of a sieve-like lamina of highly vascular connective tissue, the lamina cribrosa, whose interstices are occupied by a dense array of glial cells through which pass the RGC axons (Anderson, 1969). It has been proposed that the damaging effect of raised intraocular pressure (IOP) is associated with distortion of the lamina cribrosa, especially in its larger, peripheral interstices, and that this may impair the blood supply and/or crush the nerve fibres passing through (Anderson and Hendrickson, 1974;Quigley, 2011).

As in human and primate, the RGCs of the rat and mouse pass through a highly vascularised territory whose main constituents are a specialised type of astrocytes (the ‘glial lamina’ of (Howell, Libby, Jakobs, Smith, Phalan, Barter, Barbay, Marchant, Mahesh, Porciatti, Whitmore, Masland, and John, 2007), which we have called fortified astrocytes (FASTs; see also (Morrison, Johnson, and Cepurna, 2008)).

Rats, mice and other small rodent species, do not have a lamina cribrosa (e.g. (Morrison, Johnson, and Cepurna, 2008;Sun, Lye-Barthel, Masland, and Jakobs, 2009;Fujita, Imagawa, and Uehara, 2000;May and Lutjen-Drecoll, 2002)), but even a temporary induced elevation of IOP causes severe damage to the RGC axons at the level where they exit the eye. Is there, in these species, a different mechanism by which raised IOP damages the axons? Or can investigation of the mechanism of damage in this rat model reveal non-laminar mechanisms which are also applicable to man?

## MATERIAL AND METHODS

Adult female rats (n= 40; weight 220-250g, age 8-12 weeks) of the Albino Swiss (AS) strain (n=34), and pigmented rats of the Lister hooded strain (n= 6) were used. 12 rats were used for normal anatomy (6 AS, 6 Lister), and 28 for the glaucoma model. Apart from the presence of pigment granules no other differences were observed in the pigmented rats and they will be described together with the albinos, with the rat strain indicated in the legends of the illustrations. All animals were handled according to UK Home Office regulations for the care and use of laboratory animals, the UK Animals (Scientific Procedures) Act 1986 and ARVO Statement for the Use of Animals in Ophthalmic and Vision Research.

**Induction and measurement of raised intraocular pressure (IOP)**

Rats were deeply anaesthetized with isoflurane, and topical 0.5% proparacaine hydrochloride eye drops (Alcaine, Alcon Laboratories, Couvreur, Belgium). For unilateral induction of high intraocular pressure, 20µl of a 30mg/ml suspension of 5µm diameter magnetic microspheres (Aldehyde-terminated Magnetic, MagicBeads™, Chi Scientific) were injected into right anterior chamber and a small magnetic rod was used to direct the magnetic microspheres into the peripheral angle of the anterior chamber (Samsel, Kisiswa, Erichsen, Cross, and Morgan, 2011). IOP was recorded under general and topical anaesthesia (Jia, Cepurna, Johnson, and Morrison, 2000) using a tonometer (Tono-Pen XL, Reichert Inc, Germany) at before injection, then at 4, 7, 14, and 28 days after injection. The means ± SEM of 4 consecutive readings of IOP were 10.0±0.75mm Hg (n=28) before injection, 17.7± 0.80 (n=6) at 4 days, 20.1±1.29 (n=8) at 7 days, 24.3±3.71 (n=8) at 14 days, and 13.4±1.14 (n=6) at 28 days. In the present series of rats the IOP measurements under combined general and local anaesthesia were considerably lower than in the previous series (Dai, Khaw, Yin, Li, Raisman, and Li, 2012a) where only local anaesthesia was used.

Under deep pentobarbital anaesthesia the rats were transcardially perfused with 50ml of 0.1M phosphate buffered saline (PBS) followed by a mixture of 2% paraformaldehyde and 2% glutaraldehyde in 0.1 M PB. The ONH with adjacent tissue was dissected out and postfixed in 2% osmium tetroxide for 1-2 hours, dehydrated, and embedded in epoxy resin (TAAB, UK). Serial semithin (1.5µm) sections were cut, either longitudinally (n=18 rats), through the ONH from the retinal end to the commencement of the optic nerve, or transversely (cross-sections; n=22, rats). All sections through the series (around 300-400 cut in the longitudinal plane, and 500-600 in the transverse plane) were collected and stained with 1% methylene blue and Azur II. For electron microscopy (n=23 of these rats) ultrathin sections were cut and stained with 25% uranyl acetate in methanol for 2min and Reynold's lead citrate for 15min.

## RESULTS

### A: THE NORMAL STRUCTURE OF THE RAT OPTIC NERVE HEAD

***The specialised ONH glia: FASTs***

In longitudinal section the rat optic nerve head (ONH) is a narrow region occupying around 700µm in the antero-posterior axis. Cross sections (Fig. 1A) show an ellipse with diameters from around 250µm in the vertical plane to around 400µm in the horizontal plane, with a mid-ventral cleft containing the ophthalmic vein dorsally and the artery ventrally (Dai, Khaw, Yin, Li, Raisman, and Li, 2012b).

The FAST arrays consist of chains of elongated cells whose processes arise from around the ventral midline and radiate out to terminate around the circumference of the ONH. The FAST processes are bound into radial columns by desmosomal junctions (Hildebrand, Remahl, and Waxman, 1985), which would give mechanical stability, and gap junctions, which would provide intercellular communication, thus allowing the array to act as a functional syncytium (Malone, Miao, Parker, Juarez, and Hernandez, 2007;Quigley, 1977).

The FASTs are bound tightly to the surrounding sheath by ***surface specialisations*** which differ markedly at the ventral and dorsal circumference of the ONH. At the ***mid-ventral surface*** of the ONH the FASTs arise from large expansions, firmly anchored, like tree roots, into the surrounding dense connective tissue sheath by deeply penetrating microvilli (Fig. 1C). The microvilli are clothed by a basal lamina of around 120nm thickness, which is twice that normally found at the astrocytic glia-pial surface of the CNS. Around the crescentic ***dorsal periphery*** the FASTs terminate as a conspicuous cap (Hildebrand, Remahl, and Waxman, 1985), about 30µm in thickness, made up of a mass of short curving, finger-like processes, about 100-150nm in diameter, with highly dense cytoplasm, clothed in a glove-like fashion by a similar 120nm thick basal lamina, and inserted into the connective tissue sheath (Fig. 1B).

The striking cytoplasmic feature of the FASTs is the dense filamentous ***cytoskeleton*** (Fig. 1D; also described in the rat (Hildebrand, Remahl, and Waxman, 1985), mouse (May and Lutjen-Drecoll, 2002) and human ONH (Elkington, Inman, Steart, and Weller, 1990)). To this they owe their 'fortified' mechanical properties. The ground substance of the FAST cytoplasm is highly electron dense throughout, extending into the tips of the microvilli. In the interstices of the fibrous cytoskeleton, the FASTs have extraordinarily ***large mitochondria*** (about 0.5-1.0 µm in width) with prominent cristae giving a 'tiger stripe' appearance (Fig. 1E). The surfaces of the peripheral processes of the FASTs are abundantly supplied with pinocytotic vesicles (Fig. 1F), suggesting a fluid transport system (see below).

### *The Retinal Rim*

Scanning through a continuous series of semithin sections at the level of the opening of Bruch's membrane reveals that the junction of the ONH with the retina is encircled by a narrow rim of specialised tissue, about 20µm deep (Fig. 2A). This rim is characterised by clusters of angular, small dark cells (Fig. 2B). These cells are analogous to and continuous with the large, pale, brick-like pigment cells of the retina. As in the retina where the pigment cells lie on Bruch's membrane, the small dark cells of the rim lie on a downward turning extension of Bruch's membrane which becomes continuous with the sheath of the ONH. In the pigmented Lister hooded rats the small dark cells contain pigment granules (Fig. 2 C-G), some of which are occasionally taken up into adjacent parts of the FAST cytoplasm (Wu and Hammer, 2014).

In both the retina and the ONH the free surfaces of the pigment cells abut on a region of expanded ***extracellular spaces*** (Fig. 2C). In the retina this constitutes the subretinal space, which separates the pigment cells from the overlying photoreceptor outer segments. The continuation of this space around the retinal rim of the ONH separates the free surfaces of the ONH pigment cells from the terminals of the FAST processes. These spaces are infiltrated by extraordinary star-like villous extensions arising from the processes of the pigment cells

(Fig. 2D-F). Appropriate planes of sections show that these villi form comb-like arrays resembling those found in a renal glomerulus (Fig. 2H).

Throughout this region the apposed surfaces of the FAST processes are richly supplied with pinocytotic vesicles (Fig. 1F). Together with the giant mitochondria (Fig. 1E) and the rich array of pinocytotic vesicles on the endothelial cells (Fig. 3F, below), these arrangements suggest the anatomical correlates of a highly energy consuming fluid transport system.

Where they abut on the extracellular space the FAST processes, which are tightly apposed throughout the main body of the ONH, become separated by widening channels, like tributaries entering a lake. As will be described below the effect of a glaucomatous rise in IOP is to dam fluid back through these channels progressively splitting open the tight FAST array.

***The Vasculature***

The entire territory of the rat ONH is occupied by an extraordinarily dense, bird's nest-like tangle of microvessels (Fig. 3A). Our semithin cross sections show a vascular density of around 50 microvessel profiles per $mm^2$ (Dai, Khaw, Yin, Li, Raisman, and Li, 2012b). The input to the ONH circulation is from arteriolar branches of the posterior ciliary arteries (Morrison, 2005;Morrison, Johnson, Cepurna, and Funk, 1999;May and Lutjen-Drecoll, 2002;Hayreh, 2001) which arise from the rat equivalent of the Zinn-Haller anastomotic circle and are directed ***backwards*** into the anterior pole of the ONH (Fig. 3B,C). This backwardly directed blood flow therefore passes down the pressure gradient generated by the IOP (unlike a forward flow which would be antagonised by that gradient).

The microvessels of the ONH have a wide perivascular space containing fibroblasts and encircling fibroblastic processes (Fig. 3 D,E). This is turn is completely sealed off by a basal lamina lined wall of FAST processes. The endothelial cells have thin walls whose abluminal surface of is occupied in places by an almost continuous row of adjacent pinocytotic vesicles (Fig. 3 F, also shown in (Anderson, 1969;Hildebrand, Remahl, and Waxman, 1985)). The pinocytotic vesicles and the perivascular space are indicative of the absence of a blood brain barrier in the ONH, as has been demonstrated with HRP tracer (Flage, 1977;Kistler, Jr. and LaVail, 1981). This contrasts with the tight apposition of the perivascular astrocytic processes and fewer pinocytotic vesicles which are associated with the closed blood brain barrier in the retina, optic nerve and brain (see Fig 4 in (Dai, Khaw, Yin, Li, Raisman, and Li, 2012b)).

***The RGC axons***

The RGC axons are strikingly regular in their parallel longitudinal orientation, so that in cross sections of the ONH virtually all axons appear as circular profiles. The majority of axons are around 0.5µm in diameter with a cytoskeleton of around 30-60 microtubules, and thread-like mitochondria (an average of less than one per profile), of diameter around 0.2 µm, considerably smaller than 0.5-1.0 µm diameter 'giant' mitochondria of the FASTs.

The FAST radial processes traversing the ONH separate the axons into compartments with curving side processes further ensheathing the axons within the compartments (Fig. 4 C,I). In light of what we see in the glaucomatous ONH (below), it is significant that throughout the normal ONH there is a uniform close apposition between axons and axons and between axons

and FAST processes (Fig. 4C,I *Cf* 4J). We do not see any situations where extracellular space separates the axons from the FAST processes. We propose this close membrane-to-membrane contact allows for energy transmission from the FASTs to the RGC axons.

B: THE GLAUCOMA MODEL

We studied a rat model of glaucoma induced by temporary occlusion of the canal of Schlemm by injection of magnetic beads into the anterior chamber of the eye (Dai, Khaw, Yin, Li, Raisman, and Li, 2012b;Samsel, Kisiswa, Erichsen, Cross, and Morgan, 2011). This produced an acute rise in IOP to a peak of around 24mmHg, and started falling after 2 weeks. Although the IOP returned to close to around 13mmHg by around 4 weeks, the damage to the FASTs and the loss of axons was irreversible.

***Short term (4-7 days after raising IOP, n=14 rats):***

***A. FASTs***

At all stages after raising the IOP the robust connective tissue boundary sheath of the rat ONH remains intact and does not collapse. This is important for understanding the mechanics of the pressure induced changes within the ONH. In semithin cross sections the initial signs of damage to the ONH consist of small bleb-like areas where the FAST array is pulled away from connective tissue sheath over the dorsal surface of the ONH (Fig. 4A). These blebs are occupied by extensions of the vitreous driven by the maintained IOP to take up the space left by the retraction of the ONH tissues (see Fig. 5A below). By one week the blebs are beginning to coalesce, leading ultimately to the entire FAST array becoming detached. Electron micrographs show that the breakup of the FAST array is associated with fluid flooding into the extracellular spaces from the rim of FAST – pigment cell apposition (Fig. 4B).

Since the FAST arrays span the full width of the ONH, the detachment of the FAST processes from their dorsal circumferential attachment would have the effect of mechanically destabilising the whole array. The FAST array is firmly anchored at the ventromedial surface. As a result, the IOP acting against the rigid cytoskeleton now establishes a rotational, torque force around the pivot of the ventral base. This force is proportional to the radial length of the FAST processes. As a result, when their dorsal attachments are broken, the crescentic array of the detached FAST terminals is driven backwards by the force of the IOP acting from in front. The FAST array swings backwards like a bucket handle which is anchored by its attachments at the ventral surface with the degree of displacement increasing exponentially toward the dorsal circumference of the arc.

As increasing numbers of FAST processes detach, the diminishing numbers of remaining attachments become progressively less able to resist the undiminished deformative forces of the IOP. However, the presence of mitoses (Fig. 4C) in some of the remaining FASTs raises the possibility that the glaucomatous tissue may be able to mount a degree of regenerative response.

The detachment of the FASTs and their withdrawal from their circumferential insertions is associated with degenerative changes in the cytoplasm. The fibrous cytoskeleton loses its regular consistency, with bundles of densely stained filaments alternating in a streaky appearance with lighter stained bundles (Fig. 4D,E). The giant mitochondria lose their cristae, and become condensed into dark blurred masses (Fig. 4F,G).

***B. Axons***

Our previous study gives two views of the effects of ocular hypertension on the RGC axons – damage at the level of the ONH and damage at the level of the OpN (Dai, Khaw, Yin, Li, Raisman, and Li, 2012b).

As mentioned above, in the normal ONH there are no situations where extracellular space separates the plasma membranes of the axons from those of adjacent axons or from those of FAST processes (Fig. 4C,H). At the early stages of glaucoma, however, electron microscopy of the damaged areas around the sub-capsular dorsal circumference of the ONH reveals that the increased extracellular fluid from the region round the pigment cells now floods into the expanded extracellular spaces of the FAST array. The normally tightly apposed array of FAST processes becomes forced apart. The axons become separated from contact with the FAST processes and come to lie in expanded pools of extracellular fluid. In these areas there is a great reduction in the numbers of axons in the ONH (also reflected in our previous counts of axons in the OpN; (Dai, Khaw, Yin, Li, Raisman, and Li, 2012b)). The remaining axons are in clusters lying in contact with the FAST processes around the edges of the spaces (Fig. 4I). No axons remain lying free in the extracellular space.

Initially the axons retain their perfectly circular outlines 0.5-1.0µm in cross section, and have normal axoplasmic constituents. There is no indication that the axons are either crushed or deflected from their longitudinal orientation. With time, numbers of axons begin to show an increased number of mitochondria and in places there are large axonal swellings of up to around 15µm in diameter, containing central whorls of filaments, and peripheral areas with mitochondria and various dense bodies (Dai, Khaw, Yin, Li, Raisman, and Li, 2012b). The FAST processes of the ONH are stretched in direct contact around these axonal swellings (Fig. 4J).

***Long Term (14 and 28 days after raising IOP, n*=14 *rats)***

Longitudinal semithin sections show that by 2 weeks the former FAST array is shrunken and distorted, and has lost its connection with the sheath (Fig. 5A). The FAST processes are dark, shrivelled, and irregular, with no remnant of longitudinal orientation, and separated by wide channels of metachromatic space. The centre of the shrunken FAST array is virtually avascular. However, round its margin are what appear to be newly formed vessels characterised by thick walls and narrow lumina.

At the retinal margin the optic disc is deeply depressed with wide protrusions of vitreous which are bounded by the basal lamina of the limiting membrane of Elschnig and which extend down into the space around the shrunken FAST mass. The remainder of the space is occupied by a dense, interwoven mass of hypertrophic astrocytic processes formed by the apposition of the astrocytes of the retinal optic nerve fibre layer in front to those of the optic nerve behind. In both semithin and ultrathin sections the astrocytes are distinguished from the dark FAST processes by their pale cytoplasm. The astrocytes replace the FASTs, but they do not have any of the arrangement or specialised cytoplasmic features of FASTs (see Table 2 in (Dai, Khaw, Yin, Li, Raisman, and Li, 2012b)), although their intense GFAP staining may give the misleading impression that the normal glial structure of the ONH has survived the injury (Quigley, Addicks, Green, and Maumenee, 1981).

### *A FASTs*

Electron microscopy confirms that at the longer survivals the elegant, slender radiating FAST processes of the normal ONH become retracted into lumpy, blunt-ended structures with obvious internal signs of ongoing degradation (Fig. 5B,D). The characteristic giant mitochondria and bundles of cytoplasmic filaments have completely disappeared. The FAST cytoplasm is dark, and largely featureless, without rough endoplasmic reticulum, mitochondria, or filaments.

The metachromatic areas of the semithin sections correspond to major amounts of extracellular space occupied by redundant basal lamina and clumps of amorphous matrix (Fig. 5E). In contrast to the degeneration of the FASTs, the fibroblasts show an extraordinary degree of activation (fb and white arrows in Fig. 5B). Their cell bodies are rounded, with no longitudinal processes. The pale expanded cytoplasm contains massively expanded rough endoplasmic reticulum cisterns.

### *B Blood vessels*

Virtually no blood vessels are found in the region of the former FAST array of the ONH. Around the edges are blood capillaries showing all the signs of being new sprouts (Deane and Lantos, 1981). Unlike the normal vessels (see above) they have narrow, irregular, slit-like lumina, and thick walls with virtually no pinocytotic vesicles (Fig. 5 F,G,H). There are abundant and complex finger like protrusions into the lumen, and occasional regions where adjacent endothelial cells resemble postmitotic pairs (Fig. 5I). In places the outer wall of FAST processes surrounding the perivascular space in the normal ONH (Fig. 3D,E) is incomplete or absent (Fig. 5H).

In 3 cases the large vessels at the vitreal margin of the ONH are expanded and engorged with thrombotic material consisting of masses of platelets and red cells, with occasional lymphocytes. This indicates long term haemostasis (Fig. 5C), and suggests that the backwardly directed flow of blood has been obstructed.

There is no invasion of monocytes or any other cell type.

### *C Axons*

No normal axons are present. Occasional abnormal expanded axonal profiles with neurofilaments remain, but only in situations where they have extensive direct surface contact with FAST processes (Sx with black arrows in Fig. 4J).

## DISCUSSION

### *The fluid buffer*

By virtue of their fibrous cytoskeleton and their attachments to the surrounding thick connective tissue sheath of the ONH the radial array of FASTs provides the load bearing tissue of the rat ONH. For about 20µm from the level of the opening of Bruch's membrane the FAST processes are separated from the sheath by a rim of small dark pigment cells. These cells extend villi into glomerular-like extracellular spaces. In effect the ONH is floating as if suspended on this rim of extracellular fluid.

We propose that the elasticity of this suspension system provides a buffer to accommodate the normal fluctuations in intraocular pressure (IOP) as well as the stresses of eye movements. This is achieved by management of the fluid in the extracellular space (Fig. 6). As the IOP rises fluid extravasates from the blood vessels into interspaces around the pigment cells. As the pressure falls the fluid is re-absorbed back into the circulation (see also (Band, Hall, Richardson, Jensen, Siggers, and Foss, 2009) for a mathematical model of the effects of the pressure gradient on fluid transfer across living membranes in glaucoma).

The anatomical basis of this re-absorption is the comb like array of pigment cell villous processes projecting into the fluid spaces. Here described in the ONH for the first time, this arrangement has a marked resemblance to that in the renal glomeruli (Bloom and Fawcett, 1969). The surfaces of the adjacent FAST terminal processes are richly provided with pinocytotic vesicles, and the abluminal endothelial surfaces of the blood capillaries are also almost continuously decorated with pinocytotic vesicles. These are the structural signs of a major fluid transport system.

Movement of fluid is a highly energy dependent metabolic process, which is reflected in the presence of giant mitochondria throughout the FAST cytoplasm. The ultimate external input of energy to the system is provided by the dense network of microvessels fed by backwardly directed posterior ciliary arterioles arising from the ophthalmic artery at the level of its entry into the retina.

***The rat glaucoma model*** (Fig. 7)

We studied a rat model of acute glaucoma induced by introduction of magnetic beads into the canal of Schlemm. We propose that the glaucomatous process is set in motion when the physical demands of a maintained high IOP outstrip the energy needed to maintain the extracellular fluid buffer around the pigment cells of the retinal rim of the ONH.

In the retina the differential distribution of Aquaporin-4 along the radial axis of the Muller cell membranes (with very low incidence on the villi facing the subretinal space) indicates a transport of water away from the subretinal space towards the vitreous (Nagelhus, Veruki, Torp, Haug, Laake, Nielsen, Agre, and Ottersen, 1998). In effect this channel distribution would protect the extracellular subretinal space against expansion and retinal detachment. However, Nagelhus et al strikingly demonstrated a complete absence of aquaporins from the ONH. This would mean that the extracellular space of the retinal rim would not have this protection. Possibly this is a factor in the vulnerability of the retinal rim to water overload.

The vulnerability of the anterior peripheral rim of the ONH has also been documented clinically (Chauhan, Pan, Archibald, LeVatte, Kelly, and Tremblay, 2002), and in early experimental glaucoma in monkeys (Yang, Downs, Girkin, Sakata, Bellezza, Thompson, and Burgoyne, 2007;Downs, Yang, Girkin, Sakata, Bellezza, Thompson, and Burgoyne, 2007;Yang, Downs, Bellezza, Thompson, and Burgoyne, 2007).

Uncontrolled extravasation of fluid into the extracellular spaces of the buffering rim of pigment cells leads to fluid infiltrating the channels between the FAST processes. This expansion of the FAST array results in tearing the fine, delicate FAST processes out of the dorsal circumference of the ONH sheath (Dai, Khaw, Yin, Li, Raisman, and Li, 2012b). Since the FASTs remain anchored to the ventro-medial sheath by their stout basal processes,

a torque is set up. This puts the FAST array at a severe mechanical disadvantage. With their detached terminal processes unable to resist displacement leverage around the pivot of the fixed ventral attachment, makes the FASTs increasingly less able to resist the backwardly directed IOP, so that the increasing fluid volume is accommodated by a progressive backward displacement of the entire FAST array.

The detachment of the FASTs is accompanied by their degeneration. The giant mitochondria collapse and the filamentous cytoskeleton breaks up. Morrison et al (Morrison, 2005) also noted a loss of the gap junction protein connexin 43 (also seen in human ONH astrocytes mechanically stressed *in vitro* (Malone, Miao, Parker, Juarez, and Hernandez, 2007), which would weaken communication between the cellular elements of the remaining syncytium. Thus the FAST array is deprived both of its energy metabolism and its cohesive mechanical strength.

With time the loss of FAST tissue progresses so that the rostro-caudal length of the ONH shrinks from the normal 700µm to around 250µm at 1 week. Over the period from 2 to 4 weeks the FAST tissue of the rat ONH has virtually totally disappeared. Comparable observations of excavation of the optic nerve head in clinical glaucoma are the progressive cupping of the optic disc and thinning of the lamina cribrosa (Burgoyne, 2011;Jonas, 2011;Quigley, Hohman, Addicks, Massof, and Green, 1983).

Taken together, the detachment of the FASTs from the ONH sheath and their subsequent resorption offer an insight into the self-sustaining, progressive nature of the glaucomatous process. Once a breach has been made in the attachment of the FAST processes to the dorsal sheath two relentless factors come into play:

(1) in the ***cross sectional plane***, the remaining array becomes unstable, less able to resist pressure, and a curtain of degeneration descends from dorsal to ventral.
(2) in the ***longitudinal plane***, the decreased width of the ONH due to the loss of FASTs at the front of the ONH increases the pressure gradient across the ever dwindling amount of FAST tissue behind. Like the rungs of a ladder one layer after another of the FAST array collapses causing ever greater loading on the remaining rungs (Fig. 7).

In our 4 week samples (Dai, Khaw, Yin, Li, Raisman, and Li, 2012b) the pressure gradient across the ONH would be an order of magnitude greater than normal, even at normal IOP. This places the ever dwindling number of FASTs under ever increasing stress. Thus, as also seen clinically, the damaged system would become increasingly vulnerable to small pressure fluctuations at a level which would be tolerated in undamaged eyes (e.g. (Grant and Burke, Jr., 1982;Jonas, 2011;Morrison, Johnson, Cepurna, and Jia, 2005)).

### *A possible ischaemic factor*

But why should detachment of the FASTs cause them to degenerate? It has been suggested that the glial cells of the ONH may be directly sensitive to pressure (Balaratnasingam, Morgan, Bass, Ye, McKnight, Cringle, and Yu, 2008). ONH astrocytes have been shown to be directly affected by the mechanical stress of rising ambient pressure *in vitro* (Malone, Miao, Parker, Juarez, and Hernandez, 2007), although whether the parameters are comparable to the pressure changes inducing glaucoma *in vivo* is not clear.

The observations of ***avascularity*** of the shrunken FAST array in our material suggest another possibility for the damaging effect of raised pressure on the ONH *in vivo* is that the deformation of the FAST array prejudices their blood supply. Ischaemia of the ONH has long been proposed as a significant risk factor in the cascade of events inducing glaucoma (Hayreh, 2001;Chung, Harris, Evans, Kagemann, Garzozi, and Martin, 1999;Evans, Harris, Garrett, Chung, and Kagemann, 1999;Flammer, Orgul, Costa, Orzalesi, Krieglstein, Serra, Renard, and Stefansson, 2002;Flammer and Orgul, 1998;Hafez, Bizzarro, and Lesk, 2003;Yamamoto and Kitazawa, 1998).

We suggest that this ischaemia arises not from vascular factors operating on ocular blood flow in general, but from the specific vulnerability of the arterial supply to the ONH (Fig. 8). Because the arteries of the ONH run directly backward along the longitudinal axis of the ONH (Morrison, Johnson, Cepurna, and Funk, 1999;May and Lutjen-Drecoll, 2002;Hayreh, 2001), backward displacement of the ONH will in turn exert a dragging force on the backwardly directed arteriolar supply. The presence of congested thrombotic vessels at the retinal margin of the shrunken ONH in several rats would support the suggestion that the backwardly directed blood flow has been obstructed.

Impairment of the circulation to the ONH would further reduce the already overwhelmed energy supply, and a malignant negative feedback will come into play. Thus, further decrease of energy supply over demand will put the ever-dwindling number of FASTs under further metabolic strain (Morgan, 2000). Their collapse will result in further backward displacement, further increasing the stretching and impairment of the blood supply, and a self-sustaining vicious downward spiral of energy deprivation will come into play. In effect the damage caused by the initial imbalance erodes the mechanical framework needed to resist the IOP. Once beyond the tipping point, the process becomes irrevocable, particularly if the pressure is not controlled. Shorter increases in intraocular pressure in mice which give rise to astrocyte process retraction and shape change can result in reversal if the intraocular pressure rise is reversed (Sun, Qu, and Jakobs, 2013). In man there is clinical evidence that progression can be halted by pressure control if the disc damage and disease are not terminal.

In clinical glaucoma, such a vascular involvement is indicated by the occurrence of marginal disc haemorrhages. In the rat, however, we have seen no indication of any extravasated erythrocytes which would be a sign of haemorrhage. Nor have we seen any evidence of the recently reported transendothelial migration of proinflammatory monocytes reported in DBA/2J mutant mice (Howell, Soto, Zhu, Ryan, Macalinao, Sousa, Caddle, MacNicoll, Barbay, Porciatti, Anderson, Smith, Clark, Libby, and John, 2012). Possibly the ischaemic effect in the rat glaucoma model may be associated not with haemorrhage, but with vasospasm (Flammer and Orgul, 1998), or occlusion of stretched but intact vessels by the surrounding tissue pressure (Quigley and Addicks, 1981;Schwartz, Rieser, and Fishbein, 1977). The haemorrhages in clinical glaucoma are now thought to be a stretching phenomenon.

***Damage to the RGC axons***

During their course through the ONH the RGC axons pass through the territory of the FASTs. In the glaucomatous model the progressive withdrawal of the FAST processes from the dorsal periphery of the ONH leaves the axons denuded (Fig. 4). They are neither crushed nor distorted, but lay orphaned in wide extracellular spaces.

Counts of myelinated profiles in cross sections of the optic nerve show that the events in the ONH are accompanied by a progressive disappearance of RGC axons leading to a loss of around 80% at 4 weeks (Dai, Khaw, Yin, Li, Raisman, and Li, 2012b). The downward spiral of FAST degeneration engenders a progressive loss of axons, leading to blindness. Once this spiral has started damage becomes self-generating.

In the absence of any indication of direct mechanical damage to the axons in the ONH, why do they degenerate? In the glaucomatous ONH those axons which survive (even the occasional axons seen at longer periods) invariably have retained direct contact with FASTs (Fig. 4 I,J). This suggests that it is the withdrawal of the FAST processes, leading to loss of contact with the axons that precipitates the axonal degeneration. This would explain why the point at which the RGC axons are vulnerable to raised IOP is that part of their course where they pass through the FAST territory of the ONH (Morrison, Johnson, and Cepurna, 2008;Quigley, 2011;Howell, Libby, Jakobs, Smith, Phalan, Barter, Barbay, Marchant, Mahesh, Porciatti, Whitmore, Masland, and John, 2007;Balaratnasingam, Morgan, Bass, Matich, Cringle, and Yu, 2007;Anderson and Hendrickson, 1974;Morrison, Johnson, Cepurna, and Jia, 2005;Morgan, 2000).

But what is that support? Axonal transport, including mitochondrial translocation, maintenance of the axonal cytoskeleton and axon potentials are all highly energy (ATP) dependent. Deprivation of energy support and de-regulation of $Ca^{2+}$ homeostasis can lead to degeneration of axons (Stys, 2005;Lee, Morrison, Li, Lengacher, Farah, Hoffman, Liu, Tsingalia, Jin, Zhang, Pellerin, Magistretti, and Rothstein, 2012;Whitmore, Libby, and John, 2005;Yang, Wu, Renier, Simon, Uryu, Park, Greer, Tournier, Davis, and Tessier-Lavigne, 2015). Considerable evidence is now mounting that axons are dependent on an input of energy from the surrounding glia (Tsacopoulos and Magistretti, 1996;Barros, 2013). Mechanical stress on mouse ONH astrocytes *in vitro* and *in vivo* causes release of ATP through pannexin channels (Beckel, Argall, Lim, Xia, Lu, Coffey, Macarak, Shahidullah, Delamere, Zode, Sheffield, Shestopalov, Laties, and Mitchell, 2014).

The RGC axons have a specially high energy need. Firstly, they carry a continuous heavy traffic of action potentials since they are equally active not only when the eye is illuminated, but also in the absence of photic input (Kuffler, Fitzhugh, and Barlow, 1957;Robson and Troy, 1987). An additional factor of vulnerability is that during their course through the ONH the RGC axons are unmyelinated. Myelination begins only at the level where they enter the optic nerve proper. Unlike myelinated axons, where the $Na^+$ channels are restricted to the nodes, the highly energy demanding voltage gated $Na^+$ channels are continuous over the full length of the membranes of the unmyelinated segments of the RGC axons throughout their entire course through the ONH (Barron, Griffiths, Turnbull, Bates, and Nichols, 2004).

For both these reasons the continuously active, unmyelinated segments of the RGC axons passing through the ONH have an exceptionally energy requirement during this part of their course (Nickells, Howell, Soto, and John, 2012). This is supported by the observation that there is a huge increase in mitochondrial density in the anterior unmyelinated part of the ONH in man and other species with similar non-myelinated parts of their optic nerve (Bristow, Griffiths, Andrews, Johnson, and Turnbull, 2002).

The view that the axonal damage leading to the loss of vision in glaucoma is connected with energy deprivation is supported by the observations that pharmacological blockade of the energy dependent voltage gated Na+ channels reduces the loss of RGC axons in a rat

glaucoma model (Hains and Waxman, 2005;Stys, Ransom, and Waxman, 1992;Stys, Waxman, and Ransom, 1992) (see also (Band, Hall, Richardson, Jensen, Siggers, and Foss, 2009)) and in optic nerve axons *in vitro* (Fern, Ransom, Stys, and Waxman, 1993).

The ultimate source of energy input to neural tissues is the blood circulation, and the high energy needs of the unmyelinated RGC axon segments are reflected in the extraordinarily dense bird's nest of microvessels in the ONH. The FASTs of the ONH provide the intermediary in the transmission of energy from the rich array of blood vessels to the RGC axons. The high level of energy transfer across the FASTs is reflected in the size of the giant FAST mitochondria and the high levels of the mitochondrial marker COX IV (Barron, Griffiths, Turnbull, Bates, and Nichols, 2004).

On these grounds we propose that the damage to the RGC axons in the ONH in glaucoma is a consequence of withdrawal of the FAST processes depriving these high energy consuming axons of vital energy support.

***The Energy Theory of Glaucoma***

The ONH has to deal with continuous fluctuations in IOP, and maintained rises above a certain threshold trigger the downward spiral of glaucomatous damage. The existence of the lamina cribrosa in the human /primate ONH suggested that the energy generated by IOP is resisted by a mechanically elastic structure. In the rat, which has no lamina cribrosa, we propose that the defence against IOP is a dynamic and metabolic process. The present observation of the ONH being suspended on a ring of fluid suggests this fluid acts as a buffer to provide a flexible response to changes in IOP. As the IOP rises fluid is extravasated into the buffer and the ONH bows backwards. As the IOP falls the flow of fluid is reversed, and this allows the ONH to swing into its forward position. The re-absorption of the fluid is an energy dependent process. In effect the metabolic energy required to maintain the fluid buffer must match the mechanical energy demands on the system when the IOP rises.

The proposed sequence of events in glaucoma (Fig. 9) is:

1. The capacity of the fluid buffer is overwhelmed.
2. This leads to disinsertion of the FASTs, destabilising the array.
3. Progressive backward displacement leads to ischaemic stretching of the arterial supply.
4. Impairment of the blood supply leads to death of the FASTs.
5. And this leads to death of axons by depriving them of their energy support from the FASTs.

This theory, based on structural observations, would be supported by dynamic imaging confirming the predicted effects of IOP fluctuations on (a) the volume of the fluid buffer of the ONH rim, and on (b) on the blood flow through the backwardly directed arterial supply of the ONH.

To what extent the energy theory applies to the human/primate, and the contribution of the lamina cribrosa are the subject of studies in progress.

Finally, one might ask what purpose is served by having a mechanically resistant barrier in the ONH in rat or primate. Nerves all over the body are flexible. As with all the other cranial

nerves, as well as the brain itself, the optic nerve is in continual motion with breathing. Why not let the ONH simply ride backwards and forwards with the fluctuating intraocular pressure, and the kinetic energy be gradually dispersed along the course of the optic nerve and its dural sheath?

The key to the function of the ONH is the maintenance of unmyelinated axons. The combination of continuous neural activity and continuous sodium channels makes these axons dependent on a high energy input, which is served by backwardly directed arterioles feeding a dense mass of capillaries. Possibly in the final analysis the function of the pressure-resistant structure in the ONH is to protect this vital and delicate vasculature. And the effect of glaucoma is to tear away that protection. We propose that the primary purpose of the load bearing structure is not to protect the nerves but to protect the blood supply.

We recently presented evidence that transplanted OECs are able to ensheathe RGC axons, induce angiogenesis and reduce the degradation of the FAST array caused by raised IOP (Dai, Khaw, Yin, Li, Raisman, and Li, 2012a). We suggest that the ensheathment of the axons may preserve their vital energy input, and that the angiogenesis induced by the transplants may restore the blood supply to the remaining FASTs (Figs. 4K, 10).

ACKNOWLEDGEMENTS

Professor Xavier Golay, Head of the Department of Brain Repair and Rehabilitation at the UCL Institute of Neurology provided the key to understanding the physical and energy aspects of the system. This work was supported by grants from the UK Stem Cell Foundation and the Nicholls Spinal Injury Foundation. PTK is supported by the NIHR Biomedical Research centre at Moorfields and the Helen Hamlyn Trust & Fight for Sight. Professor Keith Martin (Cambridge, UK) and Professor James Morgan (Cardiff, UK) provided invaluable advice and encouragement. We thank Professor John Morrison (Portland, Oregon, USA) for kind permission to reproduce Figs shown in 3A,B. No authors have conflicts of interest.

Reference List

Anderson DR. 1969. Ultrastructure of human and monkey lamina cribrosa and optic nerve head. Arch Ophthal 82:801-814.

Anderson DR, Hendrickson A. 1974. Effect of intraocular pressure on rapid axoplasmic transport in monkey optic nerve. Invest Ophthalmol 13:771-783.

Balaratnasingam C, Morgan WH, Bass L, Matich G, Cringle SJ, Yu DY. 2007. Axonal transport and cytoskeletal changes in the laminar regions after elevated intraocular pressure. Invest Ophthalmol Vis Sci 48:3632-3644.

Balaratnasingam C, Morgan WH, Bass L, Ye L, McKnight C, Cringle SJ, Yu DY. 2008. Elevated pressure induced astrocyte damage in the optic nerve. Brain Res 1244:142-154.

Band LR, Hall CL, Richardson G, Jensen OE, Siggers JH, Foss AJ. 2009. Intracellular flow in optic nerve axons: a mechanism for cell death in glaucoma. Invest Ophthalmol Vis Sci 50:3750-3758.

Barron MJ, Griffiths P, Turnbull DM, Bates D, Nichols P. 2004. The distributions of mitochondria and sodium channels reflect the specific energy requirements and conduction properties of the human optic nerve head. Br J Ophthalmol 88:286-290.

Barros LF. 2013. Metabolic signaling by lactate in the brain. Trends Neurosci.

Beckel JM, Argall AJ, Lim JC, Xia J, Lu W, Coffey EE, Macarak EJ, Shahidullah M, Delamere NA, Zode GS, Sheffield VC, Shestopalov VI, Laties AM, Mitchell CH. 2014. Mechanosensitive release of adenosine 5'-triphosphate through pannexin channels and mechanosensitive upregulation of pannexin channels in optic nerve head astrocytes: a mechanism for purinergic involvement in chronic strain. Glia 62:1486-1501.

Bloom W, Fawcett DW. 1969. A Textbook of Histology. Philadelphia: W. B. Saunders Company.

Bristow EA, Griffiths PG, Andrews RM, Johnson MA, Turnbull DM. 2002. The distribution of mitochondrial activity in relation to optic nerve structure. Arch Ophthalmol 120:791-796.

Burgoyne CF. 2011. A biomechanical paradigm for axonal insult within the optic nerve head in aging and glaucoma. Exp Eye Res 93:120-132.

Chauhan BC, Pan J, Archibald ML, LeVatte TL, Kelly ME, Tremblay F. 2002. Effect of intraocular pressure on optic disc topography, electroretinography, and axonal loss in a chronic pressure-induced rat model of optic nerve damage. Invest Ophthalmol Vis Sci 43:2969-2976.

Chung HS, Harris A, Evans DW, Kagemann L, Garzozi HJ, Martin B. 1999. Vascular aspects in the pathophysiology of glaucomatous optic neuropathy. Surv Ophthalmol 43 Suppl 1:S43-S50.

Dai C, Khaw PT, Yin Z-Q, Li D-Q, Raisman G, Li Y. 2012a. Olfactory ensheathing cells rescue optic nerve fibres in a rat glaucoma model. TVST 1.2:1-12.

Dai C, Khaw PT, Yin ZQ, Li D, Raisman G, Li Y. 2012b. Structural basis of glaucoma: the fortified astrocytes of the optic nerve head are the target of raised intraocular pressure. Glia 60:13-28.

Deane BR, Lantos PL. 1981. The vasculature of experimental brain tumours. Part 1. A sequential light and electron microscope study of angiogenesis. J Neurol Sci 49:55-66.

Downs JC, Yang H, Girkin C, Sakata L, Bellezza A, Thompson H, Burgoyne CF. 2007. Three-dimensional histomorphometry of the normal and early glaucomatous monkey optic nerve head: neural canal and subarachnoid space architecture. Invest Ophthalmol Vis Sci 48:3195-3208.

Elkington AR, Inman CB, Steart PV, Weller RO. 1990. The structure of the lamina cribrosa of the human eye: an immunocytochemical and electron microscopical study. Eye 4 ( Pt 1):42-57.

Evans DW, Harris A, Garrett M, Chung HS, Kagemann L. 1999. Glaucoma patients demonstrate faulty autoregulation of ocular blood flow during posture change. Br J Ophthalmol 83:809-813.

Fern R, Ransom BR, Stys PK, Waxman SG. 1993. Pharmacological protection of CNS white matter during anoxia: actions of phenytoin, carbamazepine and diazepam. J Pharmacol exp Ther 266:1549-1555.

Ffrench-Constant C, Miller RH, Burne JF, Raff MC. 1988. Evidence that migratory oligodendrocyte-type-2 astrocyte (O-2A) progenitor cells are kept out of the rat retina by a barrier at the eye-end of the optic nerve. J Neurocytol 17:13-25.

Flage T. 1977. Permeability properties of the tissues in the optic nerve head region in the rabbit and the monkey. An ultrastructural study. Acta Ophthalmol (Copenh) 55:652-664.

Flammer J, Orgul S. 1998. Optic nerve blood-flow abnormalities in glaucoma. Prog Retin Eye Res 17:267-289.

Flammer J, Orgul S, Costa VP, Orzalesi N, Krieglstein GK, Serra LM, Renard JP, Stefansson E. 2002. The impact of ocular blood flow in glaucoma. Prog Retin Eye Res 21:359-393.

Fujita Y, Imagawa T, Uehara M. 2000. Comparative study of the lamina cribrosa and the pial septa in the vertebrate optic nerve and their relationship to the myelinated axons. Tissue Cell 32:293-301.

Grant WM, Burke JF, Jr. 1982. Why do some people go blind from glaucoma? Ophthalmology 89:991-998.

Hafez AS, Bizzarro RL, Lesk MR. 2003. Evaluation of optic nerve head and peripapillary retinal blood flow in glaucoma patients, ocular hypertensives, and normal subjects. Am J Ophthalmol 136:1022-1031.

Hains BC, Waxman SG. 2005. Neuroprotection by sodium channel blockade with phenytoin in an experimental model of glaucoma. Invest Ophthalmol Vis Sci 46:4164-4169.

Hayreh SS. 2001. Blood flow in the optic nerve head and factors that may influence it. Prog Retin Eye Res 20:595-624.

Hildebrand C, Remahl S, Waxman SG. 1985. Axo-glial relations in the retina-optic nerve junction of the adult rat: electron-microscopic observations. J Neurocytol 14:597-617.

Howell GR, Libby RT, Jakobs TC, Smith RS, Phalan FC, Barter JW, Barbay JM, Marchant JK, Mahesh N, Porciatti V, Whitmore AV, Masland RH, John SW. 2007. Axons of retinal ganglion cells are insulted in the optic nerve early in DBA/2J glaucoma. J Cell Biol 179:1523-1537.

Howell GR, Soto I, Zhu X, Ryan M, Macalinao DG, Sousa GL, Caddle LB, MacNicoll KH, Barbay JM, Porciatti V, Anderson MG, Smith RS, Clark AF, Libby RT, John SW. 2012. Radiation treatment inhibits monocyte entry into the optic nerve head and prevents neuronal damage in a mouse model of glaucoma. J Clin Invest 122:1246-1261.

Jia L, Cepurna WO, Johnson EC, Morrison JC. 2000. Effect of general anesthetics on IOP in rats with experimental aqueous outflow obstruction. Invest Ophthalmol Vis Sci 41:3415-3419.

Jonas JB. 2011. Role of cerebrospinal fluid pressure in the pathogenesis of glaucoma. Acta Ophthalmol 89:505-514.

Kistler HB, Jr., LaVail JH. 1981. Penetration of horseradish peroxidase into the optic nerve after vitreal or vascular injections in the developing chick. Invest Ophthalmol Vis Sci 20:705-716.

Kuffler SW, Fitzhugh R, Barlow HB. 1957. Maintained activity in the cat's retina in light and darkness. J Gen Physiol 40:683-702.

Lee Y, Morrison BM, Li Y, Lengacher S, Farah MH, Hoffman PN, Liu Y, Tsingalia A, Jin L, Zhang PW, Pellerin L, Magistretti PJ, Rothstein JD. 2012. Oligodendroglia metabolically support axons and contribute to neurodegeneration. Nature.

Malone P, Miao H, Parker A, Juarez S, Hernandez MR. 2007. Pressure induces loss of gap junction communication and redistribution of connexin 43 in astrocytes. Glia 55:1085-1098.

May CA, Lutjen-Drecoll E. 2002. Morphology of the murine optic nerve. Invest Ophthalmol Vis Sci 43:2206-2212.

Morgan JE. 2000. Optic nerve head structure in glaucoma: astrocytes as mediators of axonal damage. Eye (Lond) 14 ( Pt 3B):437-444.

Morrison JC. 2005. Elevated intraocular pressure and optic nerve injury models in the rat. J Glaucoma 14:315-317.

Morrison JC, Johnson E, Cepurna WO. 2008. Rat models for glaucoma research. Prog Brain Res 173:285-301.

Morrison JC, Johnson EC, Cepurna W, Jia L. 2005. Understanding mechanisms of pressure-induced optic nerve damage. Prog Retin Eye Res 24:217-240.

Morrison JC, Johnson EC, Cepurna WO, Funk RH. 1999. Microvasculature of the rat optic nerve head. Invest Ophthalmol Vis Sci 40:1702-1709.

Nagelhus EA, Veruki ML, Torp R, Haug FM, Laake JH, Nielsen S, Agre P, Ottersen OP. 1998. Aquaporin-4 water channel protein in the rat retina and optic nerve: polarized expression in Muller cells and fibrous astrocytes. J Neurosci 18:2506-2519.

Nickells RW, Howell GR, Soto I, John SW. 2012. Under pressure: cellular and molecular responses during glaucoma, a common neurodegeneration with axonopathy. Annu Rev Neurosci 35:153-179.

Quigley HA. 1977. Gap junctions between optic nerve head astrocytes. Invest Ophthalmol Vis Sci 16:582-585.

Quigley HA. 2011. Glaucoma. Lancet 377:1367-1377.

Quigley HA, Addicks EM. 1981. Regional differences in the structure of the lamina cribrosa and their relation to glaucomatous optic nerve damage. Arch Ophthalmol 99:137-143.

Quigley HA, Addicks EM, Green WR, Maumenee AE. 1981. Optic nerve damage in human glaucoma. II. The site of injury and susceptibility to damage. Arch Ophthalmol 99:635-649.

Quigley HA, Hohman RM, Addicks EM, Massof RW, Green WR. 1983. Morphologic changes in the lamina cribrosa correlated with neural loss in open-angle glaucoma. Am J Ophthalmol 95:673-691.

Robson JG, Troy JB. 1987. Nature of the maintained discharge of Q, X, and Y retinal ganglion cells of the cat. J Opt Soc Am A 4:2301-2307.

Samsel PA, Kisiswa L, Erichsen JT, Cross SD, Morgan JE. 2011. A novel method for the induction of experimental glaucoma using magnetic microspheres. Invest Ophthalmol Vis Sci 52:1671-1675.

Schwartz B, Rieser JC, Fishbein SL. 1977. Fluorescein angiographic defects of the optic disc in glaucoma. Arch Ophthalmol 95:1961-1974.

Stys PK. 2005. General mechanisms of axonal damage and its prevention. J Neurol Sci 233:3-13.

Stys PK, Ransom BR, Waxman SG. 1992. Tertiary and quaternary local anesthetics protect CNS white matter from anoxic injury at concentrations that do not block excitability. J Neurophysiol 67:236-240.

Stys PK, Waxman SG, Ransom BR. 1992. Ionic mechanisms of anoxic injury in mammalian CNS white matter: role of Na+ channels and Na(+)-Ca2+ exchanger. J Neurosci 12:430-439.

Sun D, Lye-Barthel M, Masland RH, Jakobs TC. 2009. The morphology and spatial arrangement of astrocytes in the optic nerve head of the mouse. J Comp Neurol 516:1-19.

Sun D, Qu J, Jakobs TC. 2013. Reversible reactivity by optic nerve astrocytes. Glia 61:1218-1235.

Tsacopoulos M, Magistretti PJ. 1996. Metabolic coupling between glia and neurons. J Neurosci 16:877-885.

Whitmore AV, Libby RT, John SW. 2005. Glaucoma: thinking in new ways-a role for autonomous axonal self-destruction and other compartmentalised processes? Prog Retin Eye Res 24:639-662.

Wu X, Hammer JA. 2014. Melanosome transfer: it is best to give and receive. Curr Opin Cell Biol 29C:1-7.

Yamamoto T, Kitazawa Y. 1998. Vascular pathogenesis of normal-tension glaucoma: a possible pathogenetic factor, other than intraocular pressure, of glaucomatous optic neuropathy. Prog Retin Eye Res 17:127-143.

Yang H, Downs JC, Bellezza A, Thompson H, Burgoyne CF. 2007. 3-D histomorphometry of the normal and early glaucomatous monkey optic nerve head: prelaminar neural tissues and cupping. Invest Ophthalmol Vis Sci 48:5068-5084.

Yang H, Downs JC, Girkin C, Sakata L, Bellezza A, Thompson H, Burgoyne CF. 2007. 3-D histomorphometry of the normal and early glaucomatous monkey optic nerve head: lamina cribrosa and peripapillary scleral position and thickness. Invest Ophthalmol Vis Sci 48:4597-4607.

Yang J, Wu Z, Renier N, Simon DJ, Uryu K, Park DS, Greer PA, Tournier C, Davis RJ, Tessier-Lavigne M. 2015. Pathological Axonal Death through a MAPK Cascade that Triggers a Local Energy Deficit. Cell 160:161-176.

## LEGENDS

Fig 1 *FASTs*

A Semithin section through main body of the ONH showing radial array of FASTs (Fa), A, V, ophthalmic artery and vein in mid ventral cleft. ds, location of sample of dorsal surface shown in low power EM in 1B; vs, location of sample of ventral surface shown in low power EM in 1C; Sh, sheath.
B Delicate dorsal attachment of FASTs: from the area labelled ds in A. Layer of curled up mass of delicate dorsal terminals (white arrows); s, extracellular space;
C Stout ventral attachment of FASTs (FaV). From the area labelled vs in A.
D Filamentous cytoskeleton (fil) of FAST processes. From the region of * in A.
E Giant FAST mitochondrion (M) contrasts with small axonal mitochondria (arrows).
F Pinocytotic vesicles (white arrows) on FAST processes
A, Semithin 1.5 µm thick resin cross section, methylene blue Azur II stain; B-F, Electron micrographs. X, axons. Scale bars in µm: A, 100; B,D, 1; C, 2; E, 0.5; F, 0.2.

Fig. 2 *Pigment cells and villi*

A Reconstruction of the peripheral rim (solid black, arrows) of pigment cells drawn from a continuous series of 1.5 µm thick semithin cross sections. Ophthalmic artery (A) and vein (V) occupying the median ventral sulcus of the ONH.
B Semithin 1.5 µm resin cross section of the ONH close to the retinal margin to show a segment (arrow) of the rim of dark cells in surrounding extracellular fluid space.
C Low power EM showing a segment of the surface of the ONH with pigment cells (PC) lying in extracellular space (e), and adjacent FAST terminal processes (Fa) ensheathing RGC axons (X); Sh, sheath.
D Extracellular space infiltrated by fine villous processes of pigment cells.
E Section through the superficial part of a pigment cell (pg, granules) forming a glomerular-like structure with villous processes projecting into an extracellular space (e). Adjacent capillary has thin endothelial wall decorated with an extensive row of pinocytotic vesicles (pi).
F *En face* view of a glomerulus as in E seen in a plane at right angles.
G Pigment granules illustrating different stages of maturation.
H renal glomerulus, *reproduced from Fig 30-7 (Bloom and Fawcett, 1969)*
C-G, Electron micrographs. Scale bars in µm: B, 100; C, 4; D,E,F, 1; G, 0.5; H, 0.3.

Fig. 3 *Vasculature*

A Dense, bird's nest vasculature of the ONH. *Cast reproduced with permission from (Morrison, Johnson, Cepurna, and Funk, 1999).*
B Arterial supply of the ONH vasculature, showing backwardly directed arterial branch (white arrow) of the posterior ciliary artery entering the anterior surface of the ONH. *Reproduced by permission from (Morrison, Johnson, Cepurna, and Jia, 2005).*
C Cross section of an arteriole in the ONH. The layers from inside out are endothelial cell (E), smooth muscle (SM), fibroblast (Fb), perivascular extracellular space, closed by surrounding limiting margin of FASTs (Fa).

D Cross section of normal ONH capillary showing layers as in C, but without smooth muscle.
E, Capillary showing the elongated fibroblasts in a channel of extracellular space between longitudinal FAST processes.
F High power EM to show the characteristic row of pinocytotic vesicles in the abluminal surface of the ONH capillary.
C-F, Electron micrographs. Scale bars in µm: C, 3: D,E, 2; F, 0.5.

Fig. 4 *Degeneration*

A Cross section of ONH with raised IOP showing the characteristic crescent of circumferential dorsal blebs (B) where the delicate terminals of the FASTs have been torn out of the sheath. The stout ventral processes of the FASTs remain securely inserted into the sheath (Sh) around the ventro medial cleft (V). As the optic disc is depressed, these blebs come to be occupied by a backward extrusion of the vitreous (Cf. Fig. 7)
B Low power electron micrograph showing the expansion of the subdorsal extracellular space (e) LP EM dorsal space. Cf. Fig. 1B. In this area the FAST longitudinal processes (Fa) remain inserted into the sheath by their delicate dorsal terminals (arrows).
C Mitosis (chromosomes, arrows) in a FAST process from material at early stage after raised IOP (Cf (Sun, Qu, and Jakobs, 2013).
D Normal fast filamentous processes (fil) to compare with E.
E Streaky dark/light alternation of degenerating filaments in FAST processes of ONH.
F Normal FAST giant mitochondrion to compare with G.
G Shrunken degenerating FAST mitochondria (D) with loss of internal structure.
H Normal axons to show close membrane contact with FAST processes or adjacent axons. No extracellular space. To compare with I.
I Axons associated with extracellular spaces (e) between degenerating FAST processes. The axons retain their circular outlines (as in H), indicating that they are not deflected from their strict longitudinal orientation. The axons survive in clusters where they retain contact with the FAST processes (Fa). Arrows, two shrunken orphaned axons.
J A single swollen axon segment (Sx) containing massed filaments in ONH in advanced stage of degeneration. Large portions of the axonal surface retain contact (arrows) with fine FAST processes (Fa). No axons remain in the extracellular spaces.
All cross sections.
K Re-ensheathment of an axon (X) by transplanted OEC. This is included for comparison with Fig. 4I,J in order to show how axons which have been denuded by loss of FAST processes survive when they are re-ensheathed by OECs. White arrows, encircling OEC processes; black arrows, basal lamina. This is an unpublished EM picture taken from the material in a previous study ((Dai, Khaw, Yin, Li, Raisman, and Li, 2012a); which see for details).
B-J, Electron micrographs. Survival times in days: A,C, 7 days; B,E,G,I,J, 14 days. Scale bars in µm: A,100; B,J, 2; C, 1; D,E, 0.4; F,H,I,K 0.5; G, 0.2.

Fig. 5 *Long term degeneration and angiogensis*

A Semithin longitudinal section showing depression of the optic disc. The ONH tissue (recognised at high power) is reduced to a small irregular shrunken area (white dotted outline) which is devoid of blood vessels, and has lost contact with the surrounding sheath. OpN, optic nerve. At the anterior margin the ophthalmic vein (V) is partially occluded by a thrombus (5C, below). A, ophthalmic artery.

B Degenerating, shrunken FASTs (Fa) with scant, featureless cytoplasm in wide extracellular space (e; which is metachromatic in the stained semithin section 5A) and adjacent highly activated fibroblast (Fb) with pale cytoplasm and massively expanded and swollen endoplasmic reticulum (arrows).
C Intraluminal thrombus consisting of a mass of platelets (P) and red blood cells (R). from the area marked by * in ophthalmic vein V in 5A.
D Degenerating FASTs (Fa) showing remnant of original alignment and extracellular space (e).
E Accumulation of matrix material (M) in the extracellular spaces.
F Newly formed blood vessel with thick wall (W), lumen, L.
G Newly formed blood vessel with narrow lumen (L) with surrounding fibroblast (Fb) in a perivascular extracellular space completely closed off by a glial sheath (G).
H Newly formed blood vessel with narrow lumen (L), surrounding fibroblast (Fb) and partial glial sheath (G). Asterisk, region of absent glial sheath.
I Presumed postmitotic pair of endothelial cells (E)
Indicators of angiogenesis (5F-I) would explain the increased vascularity reported in previous publication (Dai, Khaw, Yin, Li, Raisman, and Li, 2012b). B-I, Electron micrographs. Survival times, A-F,I, 15 days; G,H, 7 days. Scale bars in μm: A, 100; B,D,G,H,I, 2; C, 5; E, 0.4; F, 3. Longitudinal sections.

Fig. 6 *The principle of the fluid buffer*

Around the anterior (retinal) rim of the ONH a fluid filled space beneath the sheath is bounded by the terminal parts of the FAST longitudinal processes and the pigment cells (PC) which project villi into the space. As the IOP rises fluid extravasates into the space. As the pressure falls the villi re-absorb the fluid which is transferred through the rich array of pinocytotic pits (pin) studding the walls of the endothelial cells into the blood circulation.

Fig. 7 *Collapse of the rungs of the ladder-like FAST structure when the energy demands of a maintained high IOP overwhelm the re-absorptive capacity of the fluid buffer*.

A Upper panel: The normal arrangement of tissues at the ONH (after Lutjen Drecoll 2010 Astrocytes and Glaucomatous Neurodegeneration, Lasker/IRRF Report). Retinal layers (ret, retina; cho, choroid; scl, sclera). The radially arranged Müller cells (M) are shown as cognate to the radially arranged FASTs (F) of the ONH. The astrocytic territory of the optic nerve fibre layer is shown in green. Red asterisk, bifurcation of the ophthalmic vessels on entering the vitreous surface of the retina. ON, optic nerve, d, dura; a, subarachnoid space; s, sheath of ONH and optic nerve. The fluid buffer (blue) represents the subretinal space and its continuation into the retinal rim of the ONH. Pigment cells, yellow dots.

Lower panel: The concept of the fluid buffer. A (i) normal arrangement. (ii) increased IOP is accommodated by extravasation of fluid into the buffer extracellular space of the retinal rim on the ONH (b,b) allowing the FASTs to bend backward (down arrow) while still retaining their circumferential attachment. (iii) as the IOP falls the fluid is re-absorbed and the FAST array springs back into position (up arrow).

B Glaucomatous situation. Lower panel: As the maintained IOP (down arrows) exceeds the re-absorptive capacity of the buffer (b,b), the fluid tracks down along the circumference of the ONH tearing the FASTs away from the circumferential attachment. B lower panel iv, v, vi: one after another the rungs of the FAST array ladder (green) give way. B upper panel:

collapse of the ONH structure leads to depression of the optic disc with posterior extrusion of the vitreous (arrows).

Fig. 8 *The energy balance in glaucoma*

***Top Panel left***: the blood flow in the normotensive eye. The arterial blood flow to the eye is directed forwards from the anterior cerebral artery through the wide, thick-walled ophthalmic artery with its major branches spreading into the retina. In addition to these, the arterial circle around the optic disc feeds into two quite different destinations: (a) vessels irrigating the vast marshland of wide open, interconnecting vascular spaces of the choroid, and (b) the backwardly directed vessels feeding into the tightly configured bird's nest of microvessels in the ONH.

***Top Panel right***: as the IOP increases the ONH is depressed posteriorly and its backwardly feeding arterial supply is stretched.

The haemodynamics of the Zinn-Haller anastomotic circle is complex and may hold a key to the pathogenesis of glaucoma. How is the blood flow apportioned into these three quite different arrangements? Possibly the intra-arterial cushions of smooth muscle located at the branching of the ophthalmic artery (May and Lutjen-Drecoll, 2002) may play a regulatory role.

***Lower Panel***: the balance between the force exerted by the IOP and the energy supplied via the circulation. Under normotensive conditions the FASTs remain attached to the ONH sheath, the ONH is mechanically stable, and the energy input matches the demand. As the maintained IOP causes disinsertion of the FAST processes, the torque force makes the FAST array mechanically unstable. The effect is that the surviving FAST tissue is subjected to a proportionately greater IOP force while the further that displacement progresses the more is the energy supply is decreased by stretching and occlusion of the backwardly directed arterial supply.

Fig. 9 *The downward spiral of glaucoma*

Under equilibrium conditions raised IOP is accommodated by expansion of the fluid buffer, and this is reversed as the villi re-absorb the fluid. Once the maintained IOP overwhelms this system a downward spiral commences. The FASTs detach from the dorsal sheath and the FAST array become mechanically unstable. This stretches the backwardly running blood supply and leads to ischaemic stress and degeneration of the FASTs. This deprives the axons of energy support and they degenerate. Transplanted OECs protect the denuded axons by re-ensheathing them and inducing an angiogenic response which protects the remaining FASTs.

Fig. 10 *Axon de- and re-ensheathment*

In the normal situation the entire surfaces of the axons (circles) are always in contact either with processes of the FASTs (F) or with other axons. In the glaucomatous situation the uncontrolled extravasation of fluid separates the FAST processes and the axons come to lie orphaned in the spaces. After OEC transplant the axons are re-ensheathed by the transplanted cells, and the remaining ventral parts of the shrunken FAST processes and their ensheathed axons (asterisks) are preserved.